1992

Improving Gl Surface Joins by Using a Composite Patch

Jörg Peters

Report Number:

92-069

IMPROVING G1 SURFACE JOINS BY USING A COMPOSITE PATCH

Jorg Peters

CSD-TR-92-069
September 23, 1992

Improving G^1 surface joins by using a composite patch

by

Jörg Peters†
jorg@cs.purdue.edu

Key words: Bernstein-Bézier form, C^1 surface, tangent ratio, composite patch

Running title: Blending with composite patches

Version: September 23, 1992 **Date printed:** September 23, 1992

Submitted to: Curves and surfaces in computer vision and graphics, SPIE OE/Tech

Abstract: A popular approach to joining surface patches smoothly across a given boundary curve is to choose the transversal derivative as an average of the tangents at the end points. However, it can be observed that this type of rational linear reparametrization forces the center transversal derivatives outside the convex hull of the remaining boundary derivatives unless certain tangent ratios are equal. The result are undesirable features in the surface. To circumvent the problem a composite patch is introduced. It consists of tensor-product patches that separate the original boundary tangents, so that constant G^1 joins can be used.

† Department of Computer Science, Purdue University, W-Lafayette IN 47907
Supported by NSF grant CCR-9211322

1. Introduction

Complex surfaces have to be assembled from patches. The focus of this paper is the choice of reparametrization across patch boundaries. In particular, the effect of linearly blending the transversal derivatives on the shape of the surface is studied. A popular approach to matching patches smoothly along a given boundary is to choose the transversal derivative as an average of the tangents at the end points (see e.g. [Chiyokura, Kimura '83], [Farin '85], [Sarraga '87]). However, it can be observed (cf. Example 2.3) that this choice of reparametrization for both patches forces the center transversal derivatives outside the convex hull of the remaining boundary derivatives. The example shows that an analysis of a surface construction must not only check the solvability of the continuity constraints, but also establish bounds on the size and direction of the resulting derivatives. A closer scrutiny of the example shows that it is of particular interest to characterize the influence of the twists on the skewing or cusping of the blended surface. However, rather than experimenting with perturbations of the mixed derivatives, which off-hand results in global systems, the approach of this paper is to use a composite patch to avoid unequal tangent ratios. By covering each mesh cell with a composite patch consisting of bicubic tensor product patches, three goals are achieved. (1) The degree of the overall surface remains low. (2) There are enough degrees of freedom to enforce constant tanget ratios across all boundaries and interpolate inconsistent mixed derivatives at the vertices of a cubic mesh. (3) There are additional degrees of freedom in the interior of the composite patch.

Section 2 gives an example of the problem arising from linear blending. Section 3 discusses the composite patch construction.

2.Tangent ratios and linear smooth blending

The key concept of this section is the tangent ratio. To define this ratio, we need to review the definition of tangent plane continuity as explained for example in [Gregory '90]. Let $\square$ be the unit square and p and q two polynomial maps from $\square$ to $\mathbb{R}^3$ such that $p(\square)$ and $q(\varphi(\square))$ join along a common boundary curve in $\mathbb{R}^3$ corresponding to the parameters $(t, 0)$; φ is a map from $\mathbb{R}^2$ to $\mathbb{R}^2$ that allows us to reparametrize between the patches. If p and q form a C^1 surface piece, then, by the chain rule, there exist scalar-valued functions λ, μ and ν such that along the common boundary

$$\lambda D_1 p = \lambda D_1 q = \mu D_2 p + \nu D_2 p, \tag{E}$$

where $D_i f$ is the derivative with respect to the ith unit vector. In particular, since p and q are polynomials, λ, μ and ν can be chosen as polynomials parametrized over the interval $[0, 1]$.

(2.1) Definition. *([Faux, Pratt '79, p 215], [Sarraga '87]) The tangent ratios at the endpoints* 0 *and* 1 *of the boundary curve common to patches* $p(\square)$ *and* $q(\square)$ *are*

$$r_0 := \frac{\mu}{\nu}(0) \quad \textit{and} \quad r_1 := \frac{\mu}{\nu}(1).$$

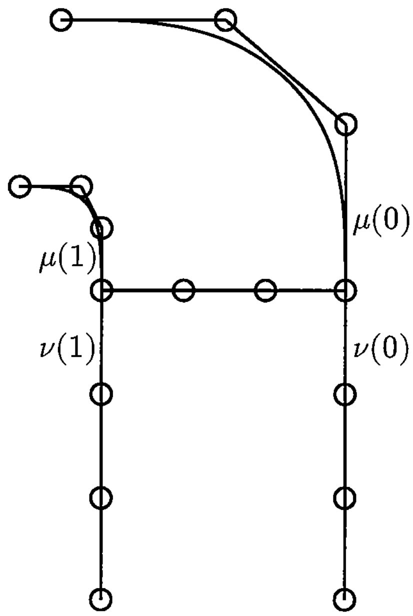

$$r_0 := \frac{\mu(0)}{\nu(0)} \neq \frac{\mu(1)}{\nu(1)} =: r_1$$

Figure (2.2) : Unequal tangent ratios [Sarraga '87, Fig. 3].

The presence of unequal tangent ratios forces surface construction algorithms to consider non constant weight functions μ and ν. The corresponding relationship between the patches is called 'geometric' smoothness in the literature and denoted by G^1. Ironically, even though many G^1 methods for generating C^1 surfaces are now known, unequal tangent ratios are still a source of trouble as the remainder of this section illustrates.

Let p and q be biquartic patches and let the common derivative $D_1 p = D_1 q$ be represented in Bernstein-Bézier (BB) form by the coefficients u_{ij}: $\sum_{i+j=3,i,j>0} u_{ij}\binom{3}{i}(1-t)^i t^j$. Let $D_2 p$ and $D_2 q$ be similarly represented by polynomials with coefficients v_{ij} and w_{ij} where $i+j=4$ and λ, μ and ν by $(\lambda_{20}, \lambda_{11}, \lambda_{02})$, (μ_{10}, μ_{01}) and (ν_{10}, ν_{01}). Setting the coefficients of each of the 6 Bernstein basis polynomials in (E) to zero yields the first-order continuity constraints

$$\lambda_{20} u_{30} = \mu_{10} v_{40} + \nu_{10} w_{40} \tag{E$_1$}$$

$$\lambda_{20} u_{21} + 2\lambda_{11} u_{30} = \mu_{10} 4 v_{31} + \nu_{10} 4 w_{31} + \mu_{01} v_{40} + \nu_{01} w_{40} \tag{E$_2$}$$

$$\lambda_{20} u_{12} + 2\lambda_{11} u_{21} + \lambda_{02} u_{30} = \mu_{10} 6 v_{22} + \nu_{10} 6 w_{22} + \mu_{01} 4 v_{31} + \nu_{01} 4 w_{31} \tag{E$_3$}$$

$$\lambda_{02} u_{21} + 2\lambda_{11} u_{12} + \lambda_{20} u_{03} = \mu_{01} 6 v_{22} + \nu_{01} 6 w_{22} + \mu_{10} 4 v_{13} + \nu_{10} 4 w_{13} \tag{E$_4$}$$

$$\lambda_{02} u_{12} + 2\lambda_{11} u_{03} = \mu_{01} 4 v_{13} + \nu_{01} 4 w_{13} + \mu_{10} v_{04} + \nu_{10} w_{04} \tag{E$_5$}$$

$$\lambda_{02} u_{03} = \mu_{01} v_{04} + \nu_{01} w_{04} \tag{E$_6$}$$

To analyze the case shown in Figure 2.2, where the end-tangents are pairwise collinear, we choose $\lambda_0 = \lambda_1 = \lambda_2 = 0$. Further, we assume that the boundary curves are prescribed and the mixed derivatives at the vertices have been determined so that (E_1), (E_2), (E_5) and (E_6) is enforced (this is the typical setup e.g. in [Sarraga '87]). Solving for the remaining coefficients of $D_2 p$ and $D_2 q$, v_{22} and w_{22}

$$6w_{22} = -r^2 w_{40} + 4r w_{31} + 4\frac{1}{r} w_{13} - \frac{1}{r^2} w_{04}$$

and by symmetry with $\rho := \frac{r_1}{r_0}$,

$$6v_{22} = -r^2\rho^2 v_{40} + 4r\rho v_{31} + 4\frac{1}{r\rho}v_{13} - \frac{1}{r^2\rho^2}v_{04}.$$

(For comparison, degree-raising a cubic with coefficents x_{ij} yields $6x_{22} = -x_{40} + 4x_{31} + 4x_{13} - x_{04}$.) We focus on the expression for v_{22}. If $\frac{||v_{04}||}{||w_{04}||} > \frac{||v_{40}||}{||w_{40}||}$ then $r_1 > r_0$ and $\rho > 1$ and the contribution of v_{04} to v_{22} is diminished while the contribution of v_{40} is increased as is desirable. However, the weighing also increases the contribution of $||v_{31}||$ and this can lead to undesirable results.

(2.3) Example Continuing the above scenario, assume for simplicity that the x and z-components of v_{22} and w_{22} are zero, but the boundary curve is not a line so that we cannot just choose all coefficients in the same plane. Then the y-components $(D_2p)^{[y]}(t,0)$ of the transversal derivative are

$$(D_2p)^{[y]}(t,0) = (1-t)^4 + 4(1-t)^3t + k_p6(1-t)^2t^2 + a4(1-t)t^3 + at^4,$$

$$(D_2q)^{[y]}(t,0) = (1-t)^4 + 4(1-t)^3t + k_q6(1-t)^2t^2 + 4(1-t)t^3 + t^4$$

for some constants k_p and k_q.

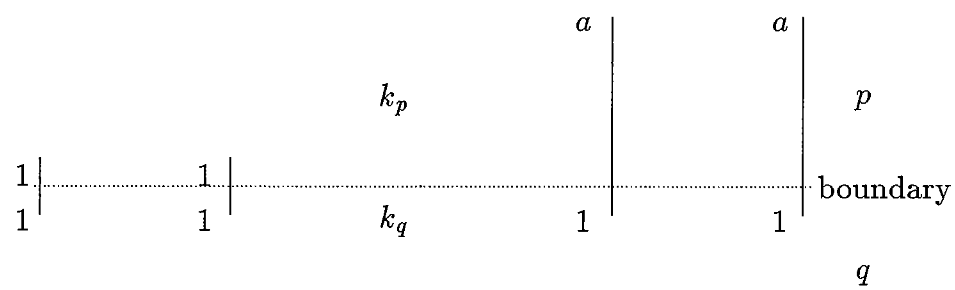

Figure (2.4) : y-components of the coefficients of the transversal derivatives.

If we fix $k_q = 1$, then

$$k_p = (a^2(4-a) + \frac{1}{a}(4 - \frac{1}{a}))/6.$$

Between $a = 4$ and $a = 6$, k_p turns negative. As shown in Figure 2.5, the transversal hodograph reverses direction for sufficiently negative values, so that two cusps develop. Such negative values for k_p can be generated for any choice of k_q. ■

The preceding example shows that the contribution of the mixed derivatives (twist coefficients) at the vertices is magnified by unequal tangent ratios under (rational) linear reparametrization. This leads to such undesirable features as cusps.

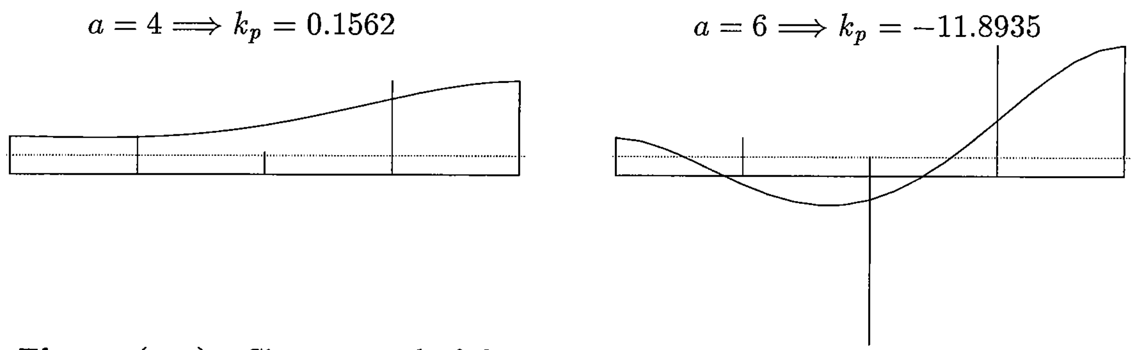

Figure (2.5) : Sign reversal of the y-component when one set of tranversal derivatives is determined by degree raising ($k_q = 1$).

3. The polynomial composite patch

The goal of the composite patch is to enforce equal tangent ratios for the C^1 construction. The technique is to split undesirable patches as illustrated in Figure 3.1: four bi-cubic patches interpolate the boundary curves while one interior bicubic (quartic) patch covers the remainder of a quadrilateral (trilateral) cell. The three different types of joins across *original* curves, *splitting* curves, and *interior* curves are labeled O, S and I. The theorem of this section states that all patches can be joined using C^1 constraints of the type

$$\lambda D_1 p = \lambda D_1 p = D_2 p + D_2 q,$$

where λ is a linear, scalar-valued polynomial. Furthermore, the construction interpolates an arbitrary mesh of cubic curves and has parameters that regulate (a) the size of the tangent plane at the original mesh nodes, (b) the orientation of the transversal derivatives across the cubic mesh curves, and (c) the location of the boundary curves of the interior patch.

(3.2) Lemma. *For any distinct set of vectors t_i, $i = 1..n$, in the plane, there exists a set of vectors T_i and constants ℓ,*

$$\alpha_i := \ell \det[t_i, t_{i+1}] \quad \textit{and} \quad \beta_i := \frac{1}{\ell} \frac{\det[t_{i-1}, t_{i+1}] + \det[t_i, t_{i+1}] + \det[t_{i-1}, t_i]}{\det[t_i, t_{i+1}] \det[t_{i-1}, t_i]} \tag{3.3}$$

such that

$$\alpha_i T_i = t_{i+1} + t_i \quad \textit{and} \quad T_{i-1} + T_i = \beta_i t_i \quad i = 1..n. \tag{3.4}$$

Proof. Substituting the first equation of (3.4) into the second yields

$$\alpha_i t_{i-1} + \alpha_{i-1} t_{i+1} = (\alpha_i \alpha_{i-1} \beta_i - \alpha_{i-1} - \alpha_i) t_i = \ell \det[t_{i-1}, t_{i+1}] t_i.$$

Substituting the above expression for α_i the result follows from Cramer's rule. ■

(3.5) Corollary. *If $\ell > 0$, then the constants α_i and β_i in Lemma 3.2 are positive if and only if* $\det[t_i, t_{i+1}] > 0$ *and* $\det[t_{i-1}, t_{i+1}] + \det[t_{i-1}, t_i] + \det[t_i, t_{i+1}] > 0$.

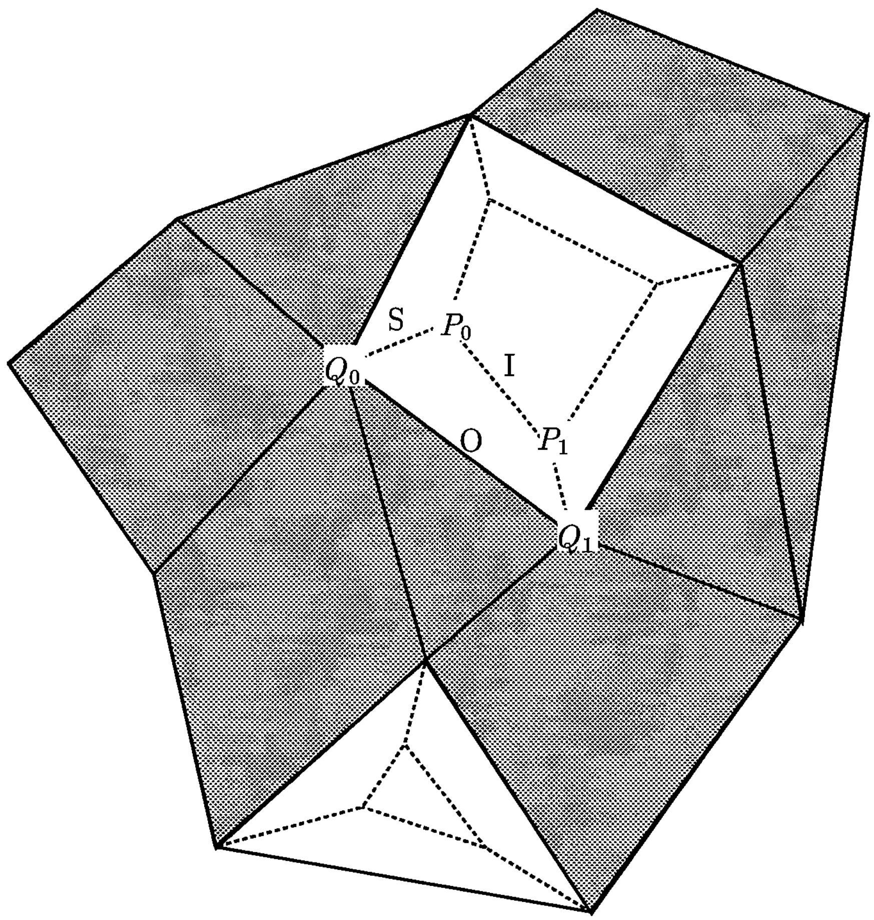

(3.1) Figure: The composite cover of a mesh cell with its three types of G^1 joins.

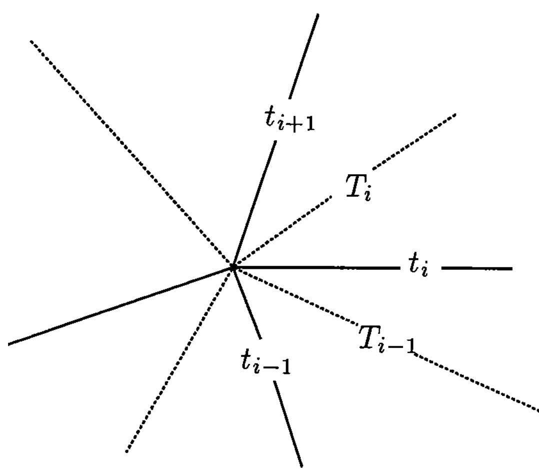

(3.6) Figure: *Old tangent vectors t_i and new tangent vectors T_i.*

To state the main theorem it is convenient to name the coefficients both with respect to the patch and globally. The coefficients of the ith boundary patch are

$$\begin{array}{rccccl} & & B_i^r & B_{i+1}^l & & \\ & & \| & \| & & \\ P_i = & b_{03}^i & b_{13}^i & b_{23}^i & b_{33}^i & = P_{i+1} \\ B_i = & b_{02}^i & b_{12}^i & b_{22}^i & b_{32}^i & = B_{i+1} \\ T_i = & b_{01}^i & b_{11}^i & b_{21}^i & b_{31}^i & = T_{i+1} \\ & b_{00}^i & b_{10}^i & b_{20}^i & b_{30}^i & \end{array}$$

where

$$Q_0 = b_{00}^i \quad b_{10}^i \quad b_{20}^i \quad b_{30}^i = Q_1$$

are the boundary coefficients that represent the given cubic boundary curve. For example, $P_i := b_{30}^i = b_{33}^{i-1}$. The double assignment is justified by the fact that the patches join continuously.

(3.7) Theorem. *Let the following data be given: a cubic mesh of curves such that the curve segments have a joint normal where they meet and such that each mesh cell has four sides. Then there exist composite patches, each covering one mesh cell with 5 patches laid out according to Figure 3.1, such that*

(1) for any two patches p and q that share a boundary curve

$$\lambda D_1 p = \lambda D_1 p = D_2 p + D_2 q,$$

along the boundary. In particular, let $u \in [0,1]$ be the parameter of the boundary curve and α_i and β_i be defined by Lemma 3.2: β_0 corresponds to $t_i := b_{10}^i - Q_0$ and β_1 to $b_{20}^i - Q_1$. Then

$$\lambda_{\mathrm{O}} = (1-u)\beta_0 - u\beta_1,$$
$$\lambda_{\mathrm{S}} = \alpha_i(1-u) + \gamma u,$$
$$\lambda_{\mathrm{I}} = -(1-u) + u.$$

For each vertex of the original mesh, there is a shape parameter ℓ; for each mesh cell, there is a shape paramete γ.

(2) The transversal derivatives of joins of type O can be chosen freely.

(3) All interior boundary coefficients, B_r^i and B_l^i can be chosen freely.

Proof. Lemma 3.2 implies a tangent ratio of 1 for curves of type O and one endpoint of the curves of type S. Hence λ_{O} is well-defiend. Examination of the C^1 constraints in terms of the BB coefficients shows that there are four constraints for each coordinate, two of which hold by the choice of the tangents at the endpoints. Each of the remaining two constraints can be solved by either of the two variables corresponding to the coefficients b_{11} and b_{12} of the two adjacent patches: for adjacent patches with labels i and j,

$$b_{11}^i + b_{12}^j = 2b_{01}^i + \frac{1}{3}\left(2\beta_0(b_{02}^i - b_{01}^i) - \beta_1(b_{01}^i - Q_0)\right) \tag{O.2}$$

$$b_{12}^i + b_{11}^j = 2b_{02}^i + \frac{1}{3}\left(-2\beta_1(b_{02}^i - b_{01}^i) + \beta_0(Q_1 - b_{02}^i)\right). \tag{O.3}$$

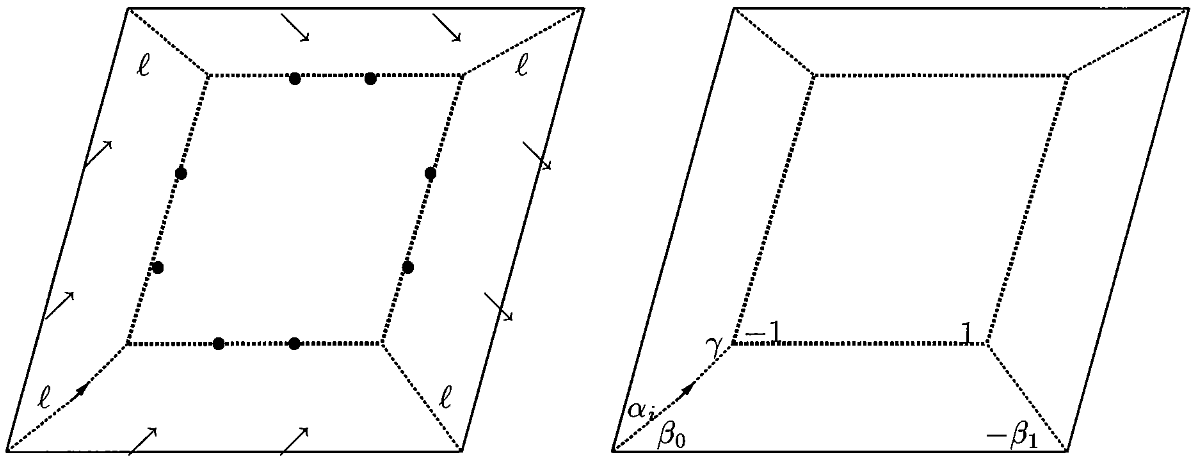

(3.8) Figure: Free parameter ↗, •, ℓ (left) and coefficients of the function λ for each of the 3 boundary types (right)

Assume that b_{11} and b_{12} are fixed for all boundary patches. At the splitting boundaries, the first of four constraints holds due to Lemma 3.2. The other three are

$$2\alpha_i(B_i - T_i) + \gamma(T_i - Q_i) = 3(b_{11}^i - T_i) + 3(b_{12}^{i-1} - T_i) \tag{S.2}$$

$$\alpha_i(P_i - B_i) + 2\gamma(B_i - T_i) = 3(b_{21}^i - B_i) + 3(b_{22}^{i-1} - B_i) \tag{S.3}$$

$$\gamma(P_i - B_i) = (b_{21}^i - P_i) + (b_{22}^{i-1} - P_i) \tag{S.4}$$

Equations (S.2) and (S.4) are enforced by setting

$$B^i = T^i + \frac{1}{2\alpha_i}\left(3(b_{11}^i - T^i) + 3(b_{12}^{i-1} - T^i) - \gamma(T^i - Q_i)\right)$$

$$P_i = B_i + \frac{1}{\gamma}(B_i^l - P_i + B_{i-1}^r - P_i).$$

Along the interior boundaries the first and the last of the four C^1 constraints are identical to Equation S.4. The remaining two require solving

$$3(M_i - B_i^r) + 3\gamma(b_{21}^i - B_i^r) = 2(B_i^r - B_{i+1}^l) + (B_i^r - P_i) \tag{I.2}$$

where M_i is the interior coefficient of the interior patch closest to P_i and the symmetric constraint I.3. The constraints S.3, I.2, and I.3 can be solved e.g. for $\gamma = 2$ by setting

$$b_{21}^i = B_i + \frac{2}{3}(B_i - T_i) + (B_i^l - B_{i-1}^r) + \frac{B_{i-1}^l - B_i^r}{6} + \frac{\alpha_i}{12}\left(\frac{B_i^l + B_{i-1}^r}{2} - B_i\right),$$

$$b_{22}^{i-1} = B_i + \frac{2}{3}(B_i - T_i) - (B_i^l - B_{i-1}^r) - \frac{B_{i-1}^l - B_i^r}{6} + \frac{\alpha_i}{12}\left(\frac{B_i^l + B_{i-1}^r}{2} - B_i\right),$$

$$M_i = B_i - \frac{4}{3}(B_i - T_i) - \frac{2}{3}\left(\frac{B_{i-1}^l + B_i^r}{2} - B_i\right) + \frac{23 - \alpha_i}{6}\left(\frac{B_i^l + B_{i-1}^r}{2} - B_i\right).$$

■

Extending the theorem to a triangular patch with quartic interior is straightforward. Next, we give default values for the three types of degrees of freedom established by the theorem. Additionally, one may use a least-squares fit to a desirable surface whose parametrization can be related to the composite patch.

1. The size of the tangent planes at the Q_i and P_i increases with the constants ℓ and γ respectively. Default choices are $\gamma = 1/2$ and $\ell = \frac{1}{3\max_i \alpha_i}$.

2. If a single patch within a fixed complex is to be 'repaired', the tranversal derivatives across the original boundaries are determined by (O.2) and (O.3). Otherwise, we can enforce strictly averaged tangents. For adjacent patches with labels i and j, this adds the constraint

$$b^i_{11} - b^j_{12} = \frac{2}{3}(b^i_{10} - b^j_{13}) + \frac{1}{3}(b^i_{13} - b^j_{10}) \tag{O$_2^*$}$$

and O_3^* which is symmetric with i and j exchanged. Together the constraints force

$$2b^i_{11} = 2b^i_{01} + \frac{2}{3}(b^i_{10} - b^j_{13}) + \frac{1}{3}(b^i_{13} - b^j_{10}) + \frac{1}{3}\left(2\beta_0(b^i_{02} - b^i_{01}) - \beta_1(b^i_{01} - Q_0)\right)$$

and similarly for the other three coefficients.

3. The 8 interior boundary coefficients are determined by computing the two Hermite interpolants to the boundary data of the original curves and subdividing at $\frac{1}{3}$ and $\frac{2}{3}$. For example, for an interior patch with four sides,

$$B^r_i = \frac{1}{27}(8b^i_{10} + 12b^i_{11} + 6b^{i+2}_{11} + b^{i+2}_{10}).$$

4. Conclusion

The example in Section 2 shows how a linear averaging of the tangents at the endpoints of a curve segment can lead to undesirable features in the transversal derivatives. The cusp appears, because the blend ignores the contribution of the mixed derivatives. This may account for the experience that forcing a surface to interpolate a mesh of unrelated boundary curves with single patches can adversely influence its shape.

The composite patch is not intended for global surface construction but rather as a tool to 'repair' a patch within an otherwise acceptable mesh of patches. Although a similar construction with triangular patches is possible, it seems preferable to construct such a composite from tensor-product patches if the original patch is quadrilateral. One can view the composite patch as a polynomial alternative to the rational corrected patch in that it can smoothly interpolate incompatible mixed derivatives at the vertices of a mesh of curves.

References

Chiyokura, Hiroaki, Fumihiko Kimura (1983), Design of Solids with Free-form Surfaces, *Computer Graphics*, **17**, No. 3, 289-298.

Farin, Gerald (1985), A modified Clough-Tocher interpolant, *Computer Aided Geometric Design* **2**, 19–27.

I.D. Faux and M.J. Pratt (1979), "Computational geometry for design and manufacture", Ellis Horwood.

J.A. Gregory (1990), Smooth parametric surfaces and n-sided patches, *Computation of curves and Surfaces*, W. Dahmen, M. Gasca and C.A. Micchelli, eds., Kluwer Academic Publishers, Dordrecht, 1990: 457–498.

R.F. Sarraga (1987), G^1 Interpolation of Generally Unrestricted Cubic Bézier curves, *CAGD* 4(1-2):23–40,1987